Jurnal Teknologi

Full paper

Water Content Estimation in Soils Using Novel Planar Electromagnetic Sensor Arrays

Mohd Amri Md Yunus[a*], Syahrul Hisyam Mohamad[b], Alif Syarafi M. Nor[a], Muhammad Hafis Izran[a], Sallehuddin Ibrahim[a]

[a]*Process Tomography and Instrumentation Engineering Research Group (PROTOM-i), Infocomm Research Alliance, Faculty of Electrical Engineering, Universiti Teknologi Malaysia, 81310 UTM Johor Bahru, Johor, Malaysia*
[b]*Faculty of Engineering Technology, Universiti Teknikal Malaysia Melaka, Ayer Keroh, Melaka*

*Corresponding author: amri@fke.utm.my

Article history

Received :30 April 20132
Received in revised form :
9 July 2013
Accepted :5 August 2013

Graphical abstract

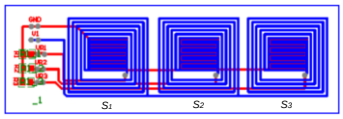

Abstract

Agriculture is one of the important sectors for food supplies. Therefore, a tool for monitoring the agro-environment is important in order to maintain the permanence of agricultural soils. This paper suggests an alternative method for the detection of water content in soils by developing a sensor array with a combination of planar meander and interdigital electromagnetic sensors. The study involved sensor array fabrication using the printed circuit board (PCB) method. The experimental setup consisted of a frequency waveform generator and a signal oscilloscope to collect and analyse the sensors' output, with VEE Agilent software used to establish the interface. A set of experiments was conducted to determine the relationship between the sensors' output and the soils' parameters. The performance of the system was observed where the sensors were tested with the addition of various kinds of soil samples with different concentrations of water content. The sensitivity of the developed sensors was evaluated where the best sensor was selected. Based on the outcomes of the experiments, the Y sensor array placement has the highest sensitivity and can be used to measure the water content in the soils where the data accuracy is compared

Keywords: Water content estimation in soils; planar electromagnetic sensor array; interdigital; meander

1.0 INTRODUCTION

The development of sensors and transducers is an urgent need as they are the key components in ensuring the operational success of any industry sector. Research outcomes show that sensors and transducers have a significant influence on the industrial sector globally [1]. In recent years, environmental awareness has become one of the principals in technological and industrial development, thus making environmental monitoring technologies a substantial, high-technology business opportunity. Environmental sensors come in literally thousands of forms and types, based on a wide range of physical and chemical principles, with varying types of usable outputs. Typical components monitored are the water content in water, metals, volatile organic compounds, biological contaminants and radioisotopes.

Soil is a valuable key natural resource; while 29 % of the world is cover by land, the other 71 % is primarily ocean. Soil has a very important role in supporting life and is a major prerequisite for sustainable development in terrestrial environments. Natural background concentrations in soils have been altered significantly by anthropogenic activities; especially in regions where agricultural, industrial and mining land uses are practised [2]. The content of the soil has direct effects on the ecosystem. Hence, long-term sustainability of food production requires improved understanding and monitoring of the soils' content [3]. Ambient background concentration data are highly voluble with potential uses such as bioavailability, toxicity and development of sites.

Technological constraint is also one of the factors that has become a hindrance to agro monitoring, although there are many methods, such as chromatography techniques [4–8], surface plasmon resonance (SPR) [9–12], enzyme-linked immunosorbent assay (ELISA) [13–17], UV-spectroscopy [18], sensor arrays [19], photo acoustic sensors [20], mass spectrometry [21], biosensors [22], bio-optoelectronics [23] and acoustic plate mode sensors [24], which can be used to estimate the components in soils, including water, but all the methods suffer from various drawbacks. The most common drawback within these detection methods is that they often involve laborious measuring steps causing the detection process to take a long time to complete.

In relation to the drawbacks and the hindrances of the detection methods mentioned above, there is a need to develop a sensor which can be integrated at low cost, is convenient and suitable for an in-situ measurement system for soil quality monitoring, and maintains the permanence of the soils. Planar electromagnetic sensors can provide an alternative where they have been proven to be low cost, require fewer components to operate, are durable, and are widely used in non-destructive testing and property estimation [25–27]. Therefore, this research is motivated

by assessing the feasibility of new applications of planar electromagnetic sensors in estimating the level of water content in soils.

2.0 EXPERIMENTAL SET-UP

2.1 Basic Design of Planar Electromagnetic Sensors

Planar electromagnetic sensors can be characterized as one of the non-destructive testing (NDT) sensors due to the operation of the sensor which does not harm the material under test. Planar electromagnetic sensors are mainly used in the detection of near-to-the-surface properties, such as dielectrics, permeability and conductivity. The best applications of the planar electromagnetic sensor are determined by the chosen sensor and tested material characteristics. There are two types of planar electromagnetic sensor: the inductive type and the capacitive type.

2.2 Meander and Interdigital Planar Electromagnetic Sensors

The meander planar electromagnetic sensor is categorized as an inductive planar electromagnetic sensor. Typically, it consists of two coils, with the coils perpendicular to each other in position. The two coils are known as the exciting coil. In addition, there is a secondary coil known as the sensing coil. The exciting coil is connected to the power source and carries the alternating current and, due to that current, the exciting coil generates a high frequency electromagnetic field. The generated high frequency electromagnetic field penetrates the material under test. Given that the material under test is of the magnetic or conducting type, the induced electromagnetic field in the testing system generates an eddy current on the material under test. Due to the eddy current flow generated inside the material under test, the corresponding induced field in the testing system modifies the generated field. The resultant field is detected by the sensing or pick coil which is placed above the exciting coil [25]. The meander sensor can be seen in Figure 1. The planar meander and mesh type sensor have been used in the inspection of a defect in connection with a printed circuit board (PCB) and have also been use in the inspection of material defects, such as the existence of inner layer cracks and for the estimation of fatigue in metal products [26].

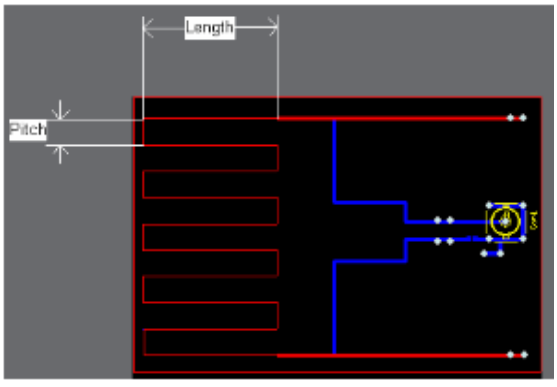

Figure 1 Configuration of meander planar electromagnetic sensors

Another configuration of the planar electromagnetic sensor is the interdigital configuration. The operating principle of the planar interdigital sensor follows the rule of two parallel plate capacitors, where, in this condition, the electrodes are open to provide one-sided access to the material under test. The basic design of the interdigital sensor, the electric field lines of the parallel plate capacitor and an interdigital sensor are shown in Figure 2. The electric field lines generated by the sensor penetrate into the material under test and change the impedance of the sensor. The sensor behaves as a capacitor in which the capacitive reactance becomes a function of the system properties. Therefore, by measuring the capacitive reactance of the sensor the system properties can be evaluated.

Since the electrodes of an interdigital sensor are coplanar, the measured capacitance will have a very low signal-to-noise ratio. In order to get a strong signal, the electrode pattern of the interdigital sensor can be repeated many times. The term "interdigital" refers to a digit-like or finger-like periodic pattern of parallel in-plane electrodes, used to build up the capacitance associated with the electric fields that penetrate into a material sample. The conventional interdigital sensor is shown in Figure 3. An AC voltage source is applied as the excitation voltage between the positive terminal and the negative terminal. An electric field is formed from the positive terminal to the negative terminal.

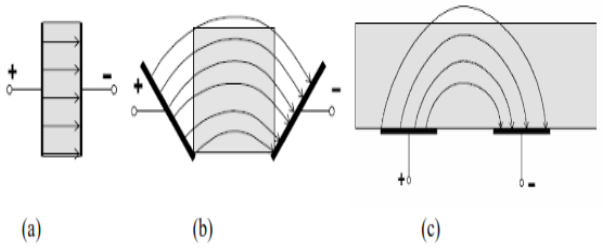

Figure 2 Electric field lines of (a) Parallel plate capacitors (b) Slanted parallel plate capacitors (c) Planar interdigital sensors

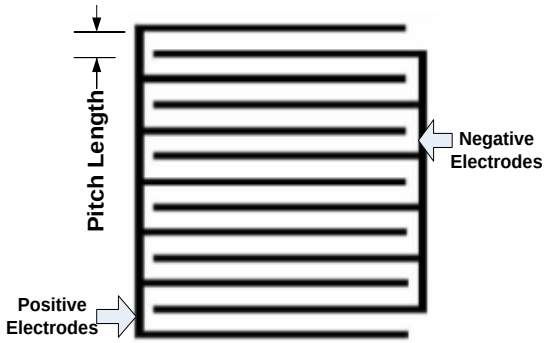

Figure 3 Conventional interdigital sensor

Figure 4 shows the side view of the interdigital sensor, showing how the electric field was formed between the positive and negative electrodes. It shows clearly that the penetration depths of the electric field lines vary for different pitch lengths. The pitch length of the interdigital sensor is the distance between two consecutive electrodes. Also, in Figure 4, there are three pitch lengths (l1, l2, and l3) showing the different penetration depths with respect to the pitch length of the sensor. The penetration depth can be increased by increasing the pitch length, but the electric field strength generated at the neighbouring electrodes will be weak [26].

2.3 Meander and Interdigital Planar Electromagnetic Sensors

The design of the sensor is based on a combination of the meander sensor and the interdigital sensor. The sensor design was carried out on the Altium Designer Summer 09. Each sensor on the sensor array has a top and a bottom. The top consists of a square spiral

meander, enclosing an interdigital sensor, where the meander sensor is connected in series with the interdigital sensor [27]. In order to increase the strength of the magnetic field, the meander number of the meander loop was set at five turns [28, 29]. The bottom is the ground plate which acts as a backplane of the interdigital sensor to keep the electric fields on the top [27]. The designs of the top and bottom of the sensor can be seen in Figure 5. In order to increase the overall sensitivity of the sensors, three types of sensor array were suggested based on electrical circuit configurations. The suggested placements were parallel placement, delta placement, and Y placement.

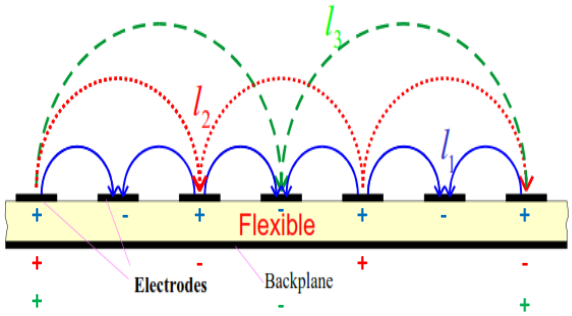

Figure 4 Electric field formed between positive and negative electrodes for different pitch lengths, (l_1, l_2, and l_3)

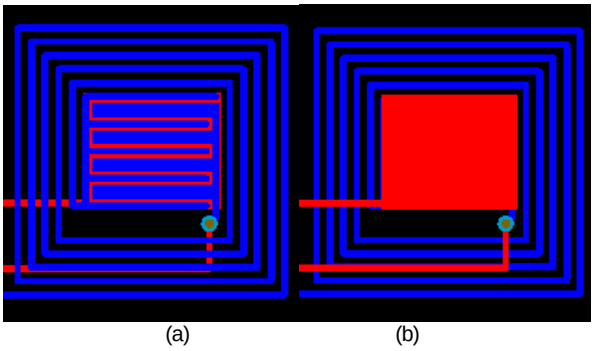

Figure 5 The planar electromagnetic sensor design a) Top b) Bottom

Each sensor on the sensor array consists of a combination of the planar meander sensor and the interdigital sensor. The overall dimensions of the meander sensor are 20 mm × 20 mm with five square loops. The distance between any outer loop and the neighbouring inner loop is 0.5 mm. With regard to the interdigital sensor design, the sensor had five positive electrodes and four negative electrodes. The widths of the positive and negative electrodes were set at 0.5 mm and 1.0 mm, respectively. The design can be found in Figure 5. An interdigital sensor with wider negative electrodes proved to improve the overall response in [28, 29]. The ground plate was located at the bottom and under the interdigital sensor; the ground plate dimension size was 8 mm × 10 mm.

Figure 6 shows the overall design of the parallel sensor array and the locations of the sensors, S_1, S_2, and S_3, which are connected in parallel with the input source signal. The distance between two neighbouring sensors is 10 mm. The top is marked in blue showing the connection of the planar meander and the interdigital sensors, while the bottom is marked in red showing the connection of the ground backplane. The surface mount device (SMD) resistors, R_1 (120 kΩ), R_2 (120 kΩ), and R_3 (120 kΩ), are connected in series with S_1, S_2, and S_3, respectively, through the ground. The output voltage for each sensor is measured. The output voltages for S_1, S_2, and S_3 are V_{R2}, V_{R3}, and V_{R3}, respectively. The input voltage is marked as V_1. The overall dimensions of the sensor are 80 mm long by 47 mm wide.

The design of the Y sensor array is shown in Figure 7. The difference between the parallel sensor array and the Y sensor array is only the placement of the S_1, S_2, and S_3 sensors. The Y sensor array design shows that S_2 is located 45° from S_1 and S_3 is located -45° from S_1. S_2 and S_3 are separated by an angle of 90° as shown in Figure 7.

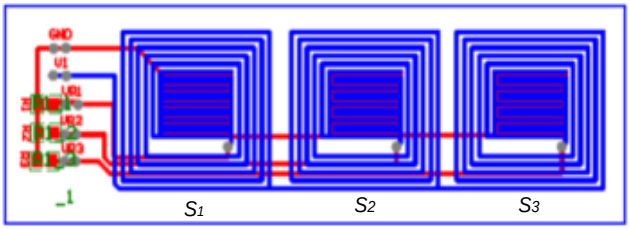

Figure 6 Design of parallel sensor array based on the combined meander sensor and interdigital sensor

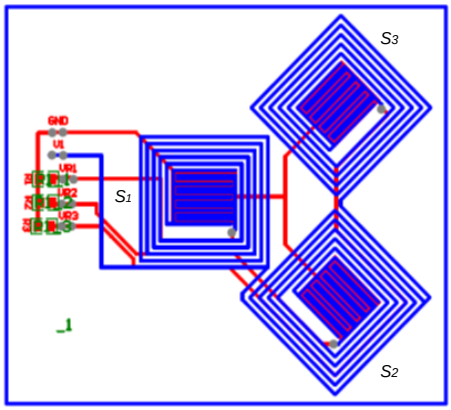

Figure 7 Design of Y sensor array based on the combined meander sensor and interdigital sensor

The delta sensor array comprised the same S_1, S_2, and S_3 sensors. The format of the delta sensor array can be seen in Figure 8. S_2 is set as the reference and S_1 is placed -45° from the top of S_2 and S_3 is placed 45° from the top of S_2. S_1 and S_3 are separated by an angle of 90°.

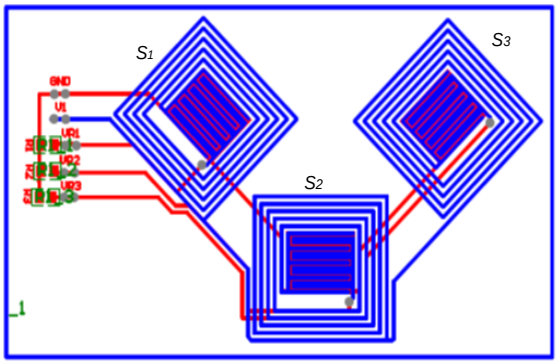

Figure 8 Design of delta sensor array based on the combined meander sensor and interdigital sensor

3.0 EXPERIMENTAL SETUP

In order to investigate the characteristics of the new sensor arrays, an experimental setup was established. It consisted of development hardware and software. For the hardware, the function of the frequency waveform generator was to give an input signal to the sensor array for the generator to generate a sinusoidal waveform with 10 Volts peak-to-peak with a frequency range between 100 kHz and 1 MHz. A modular PC integrated oscilloscope was used to detect and measure the output of the signal. Agilent VEE Pro 9.3 software was used to analyse the sensors' output. The output signals and the sensors' impedance were recorded and calculated consecutively using the developed programs. The experimental setup is shown in Figure 9.

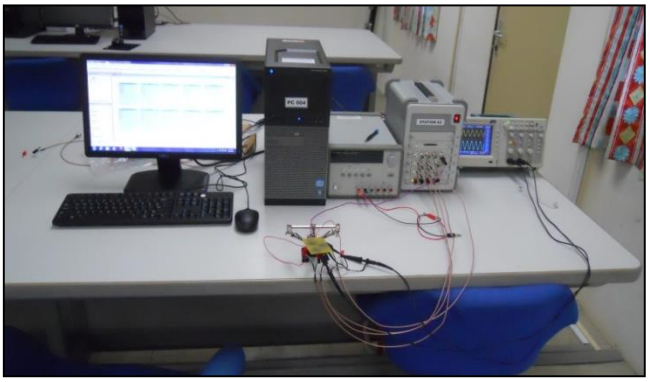

Figure 9 Experimental setup

4.0 RESULTS AND DISCUSSION

4.1 Principle of Measurement

For each sensor on the sensor array, the sensor's output impedance was analysed to obtain the characteristics of the sensor. The process was repeated when the water level within the soils was increased. The equivalent circuit for the planar electromagnetic sensor array (parallel sensor array, Y sensor array, or delta sensor array) is shown in Figure 10.

The real, R, and imaginary, X, are calculated for each of the sensors on every sensor array. Based on the equivalent circuit, R, real and X, imaginary, can be calculated from Equations (1) to (9), where I_{R1}, I_{R2}, and I_{R3} are the rms values of the current through S_1, S_2, and S_3, respectively. V_{R1}, V_{R2}, and V_{R3} are the rms voltage values across the surface mount resistor R_1, R_2, and R_3, respectively. V_1 input is considered as the reference so that its phase angle is 0 and θ is the difference in phase between the input voltage and the voltage across the resistance. The real and imaginary values can be found from the following formulas:

$$I_{R1}\angle\theta_1 = \frac{V_1}{R_1} \tag{1}$$

$$I_{R2}\angle\theta_2 = \frac{V_2}{R_2} \tag{2}$$

$$I_{R3}\angle\theta_3 = \frac{V_3}{R_3} \tag{3}$$

The currents that flow through S_1, S_2, and S_3 are I_{R1}, I_{R2}, and I_{R3}. From this we can ascertain that the polar form of impedance can be found from:

$$Z_1\angle\theta_1 = \frac{V_1}{I_{R1}}\angle\theta_1 = \frac{V_1\angle\theta_1}{V_{R1}} * R_1 \tag{4}$$

$$Z_2\angle\theta_2 = \frac{V_1}{I_{R2}}\angle\theta_2 = \frac{V_1\angle\theta_2}{V_{R2}} * R_2 \tag{5}$$

$$Z_3\angle\theta_3 = \frac{V_1}{I_{R3}}\angle\theta_3 = \frac{V_1\angle\theta_3}{V_{R3}} * R_3 \tag{6}$$

where:

I_{R1} is the current flow through S_1;
I_{R2} is the current flow through S_2;
I_{R3} is the current flow through S_3;
$Z_1\angle\theta_1$ is the impedance magnitude and phase for S_1;
$Z_2\angle\theta_2$ is the impedance magnitude and phase for S_2;
$Z_3\angle\theta_3$ is the impedance magnitude and phase for S_3.

Therefore, for S_1, S_2, and S_3, the real value and the imaginary value are given by

$$R = Z * \cos\theta \tag{7}$$

$$X = Z * \sin\theta \tag{8}$$

The total impedance can be ascertained from:

$$Z = \sqrt{(R)^2 + (X)^2} \tag{9}$$

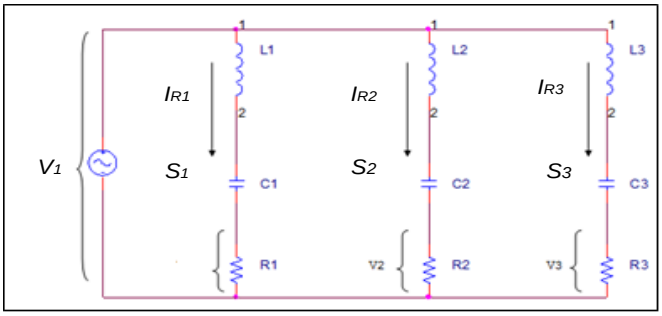

Figure 10 Equivalent circuit of the planar electromagnetic sensor array

Initial experiments were undertaken to study the characteristics of the sensor in the open air condition. The experiment was carried out by supplying the sensor's input, V_1, with a sine wave 10 V peak-to-peak and the frequency was increased logarithmically starting from 1 Hz to 1 kHz. The results of the impedance characteristics in the open air are shown for the parallel sensor array (Figure 11), Y sensor array (Figure 12) and delta sensor array (Figure 13). Based on the graphs in Figures 11, 12, and 13, it can be concluded that all sensors in any sensor array type are capacitive between the frequencies 1 kHz to 50 kHz, where, at that range, the impedance value is decreasing when the frequency value is increasing. Starting from a frequency of 150 kHz and above, the sensors' impedance values reach resonant frequency where the real value of the impedance is at the maximum range.

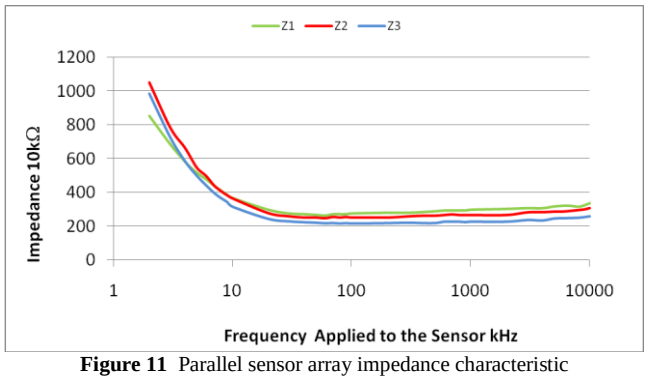

Figure 11 Parallel sensor array impedance characteristic

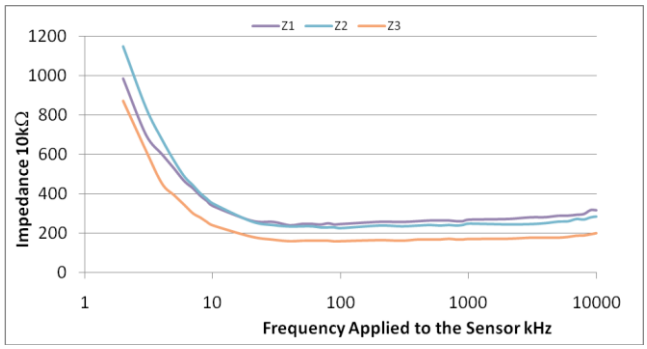

Figure 12 Y sensor array impedance characteristic

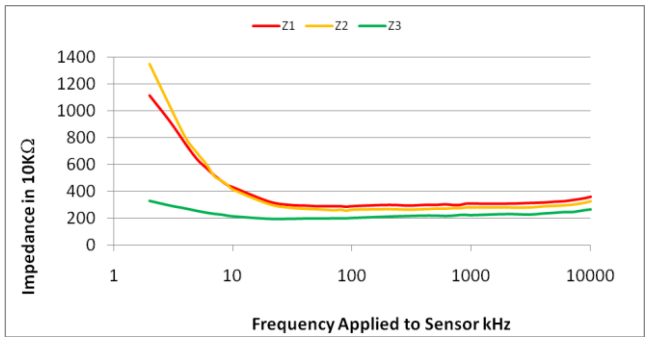

Figure 13 Delta sensor array impedance characteristic

4.2 The Responses of the Planar Electromagnetic Sensor Arrays with Different Ratios of Water Level

The sensor arrays were tested with different ratios of water in the soil. The experimental work was carried out in the laboratory using Agilent VEE 9.3 Pro software to establish the interface. The first process was completed by measuring the characteristics of the dried soils for all three sensor arrays. The weights of the soils were then measured and the characteristics of the impedance of the sensors were recorded. The sensor was placed under the soils' plastic packs, without direct contact with the soils. In order to see the relationship of the water level in the soils, an amount of water was added to the soils gradually based on the percentage of the soil. Every time before and after the water was added to the soil, the weight of the soil was taken. The water content can be measured based on Equation (10):

$$water\% = \frac{mass\ of\ water}{(mass\ of\ soils\ \ with\ \ water\ \ addded) + (mass\ of\ water)} \times 100 \quad (10)$$

Based on the condition of the sensor arrays tested with air, the sensor arrays are mostly capacitive. It was also discovered that the resonant frequency of the sensor is within 100 kHz up to 10 MHz where the $R >> X$. The next experiment was carried out to monitor the effect of the water percentage on the result of the sensor in the range of 100 kHz to 10 MHz. All sensor arrays were tested with the same soil origins with water added to the soil according to the percentage weight of the soil.

The outcomes of the experiments show that the sensor works best at a frequency of 600 kHz. The results of the experiments on the sensors with different mixes of water percentage added to the soil can be seen in Figures 14, 15 and 16 for the parallel, Y and delta sensor array placements, respectively.

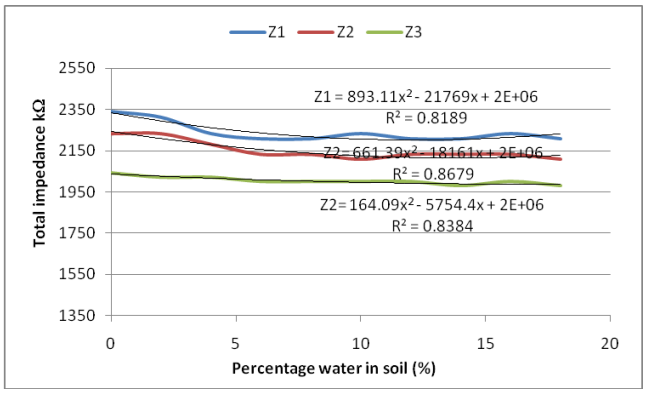

Figure 14 Parallel sensors array impedance against water percentage (%) response at 600 kHz

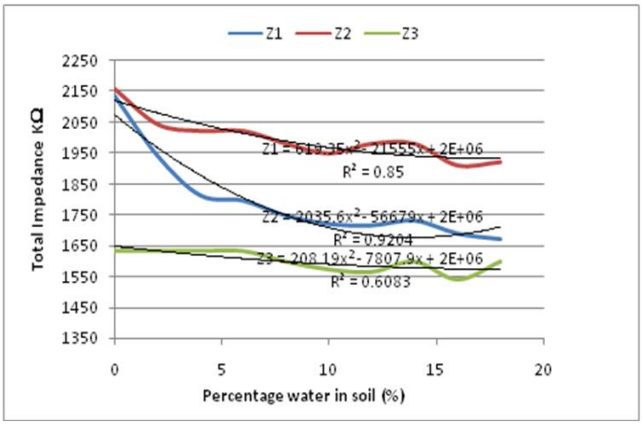

Figure 15 Y sensors array impedance against water percentage (%) response at 600 kHz

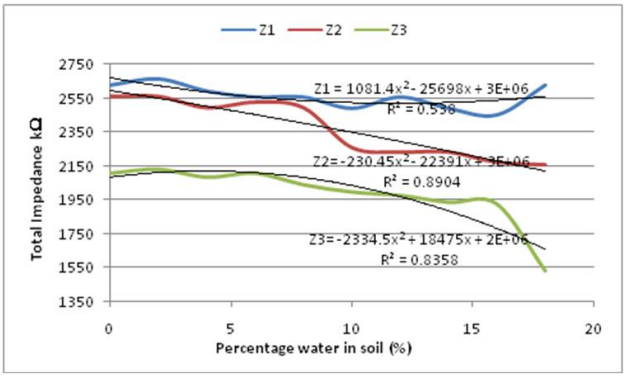

Figure 16 Delta sensors array impedance against water percentage (%) response at 600 kHz

The sensors' characteristics show that all the responses of the sensors on the sensor arrays are best fitted with polynomial trend lines. The graph in Figure 14 shows consistent correlation with R^2 = 0.8189, R^2 = 0.8679, and R^2 = 0.8384, respectively, between S_1, S_2 and S_3's impedance with the percentage of water in the soils. Meanwhile, significant increments and decrements of the correlation values for S_1's Y sensor array and S_2's delta sensor array are shown in Figures 15 and 16, respectively. On the whole, the delta sensor array showed significant water level detection in the soils where the sensors on the delta sensor array were able to discriminate between low and high percentage values of water content in the soils, as shown in Figure 16. Next, the sensitivity of the real part of the sensor is calculated, where the real sensitivity is given by Equation (11):

$$\%R = \frac{R_{soil} - R_{air}}{R_{air}} \times 10C \quad (11)$$

where:

R_{soil} is the real part value when water is added;
R_{air} is the reference value for real part (i.e. when the sensor is in air).

For the real output for the sensor arrays, the water added to the soil will change the conductivity of the soil. In theory, the conductivity of the soil will increase when with the increase in the percentage of water. In turn, it will cause an increase in the electromagnetic induction (eddy currents). The changes are then detected by every sensor on the sensor array. These changes are then converted into the real (R) changes in the sensor. The effect of the different levels of water percentage to the real sensor can be seen in Figure 17. The analysis of the sensor shows that, for the parallel array, the S_1, S_2, and S_3 real sensitivity values decrease with the increasing water level; however, the sensitivity values are saturated at around 160 ml of water volume. It can be concluded that the real sensitivity of the parallel sensor arrays is moderate towards the addition of water. The parallel array sensors could not generate electromagnetic fields to induced eddy currents in the soils.

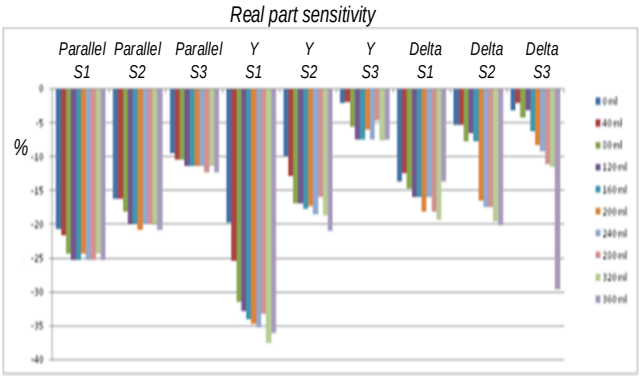

Figure 17 Sensitivity of real sensors to the different levels of water in the soils.

From Figure 17, S_1's real Y sensor array is has the most significant sensitivity changes to soil contamination levels followed by S_2. S_3 is seen to be the least responsive to the changes in water content in the soils. S_1 and S_2 decrease with the polynomial fit with the changes shown in Figure 17.

For the delta sensor array, it can be seen that the real sensor changes almost linearly for sensor S_1. However, the trends have changed to polynomials for sensors S_2 and S_3. It can be seen that the real sensitivity of S_1 is better than that of S_2 and S_3. The design of the sensor has an influence on the real sensitivity, where S_1 is nearest to the power supply followed by S_2 and S_3.

5.0 CONCLUSION

In the world's ecosystem, soil plays an important role in supporting life and is a major requirement to maintain sustainable development in terrestrial environments. In today's situation, soils are degrading in terms of quality due to uncontained human activities. As a result, planar electromagnetic sensors are seen as a rising technology in the context of detecting contamination within soil due to the ease of design, ease of fabrication and the low cost.

From the outcome of the experiments, it can be said that all the planar electromagnetic sensor arrays can detect the different levels of water content in the soils. However, all the sensors have different profiles and the Y sensor array has the highest sensitivity. In order to ensure better sensitivity for all sensors, the power track lines need to be as short as possible, thus reducing possible stray electromagnetic production. In the future, advance signal processing methods, such as independent analyses, need to be applied to the output of the sensor to improve the analysis.

Acknowledgement

The authors would like to acknowledge the Exploratory Research Scheme Grant (ERGS) from the Ministry of Higher education Research (MOHE) Malaysia (Vote No. 4L039) and Universiti Teknologi Malaysia, Research University Grant Scheme (Vote No. 08J88).

References

[1] P. D. Andersen, B. H. Jørgensen, L. Lading *et al*. 2004. Sensor Foresight-Technology and Market. *Technovation*. 24(4): 311–320.
[2] K. Sultan, and N. A. Shazili. 2009. Distribution and Geochemical Baselines of Major, Minor and Trace Elements in Tropical Topsoils of the Terengganu River Basin, Malaysia. *Journal of Geochemical Exploration*. 103(2–3): 57–68.
[3] M. Abat, M. J. McLaughlin, J. K. Kirby *et al*. 2012. Adsorption and Desorption of Copper and Zinc in Tropical Peat Soils of Sarawak. Malaysia. Geoderma. 175–176: 58–63.
[4] V. Andreu, E. Ferrer, J. L. Rubio *et al*. 2007. Quantitative Determination of Octylphenol, Nonylphenol, Alkylphenol Ethoxylates and Alcohol Ethoxylates by Pressurized Liquid Extraction and Liquid Chromatography–mass Spectrometry in Soils Treated with Sewage Sludges. *Science of the Total Environment*. 378(1–2): 124–129.
[5] S. R. Rissato, M. S. Galhiane, M. V. de Almeida *et al*. 2007. Multiresidue Determination of Pesticides in Honey Samples by Gas Chromatography–mass Spectrometry and Application in Environmental Contamination. *Food Chemistry*. 101(4): 1719–1726.
[6] H. Van De Weghe, G. Vanermen, J. Gemoets *et al*. 2006. Application of Comprehensive Two-dimensional Gas Chromatography for the Assessment of Oil Contaminated Soils. *Journal of Chromatography A*. 1137(1): 91–100.
[7] G. L. Hook, G. Kimm, D. Koch *et al*. 2003. Detection of VX Contamination in Soil Through Solid-phase Microextraction Sampling and Gas Chromatography/mass Spectrometry of the VX Degradation Product bis(diisopropylaminoethyl)disulfide. *Journal of Chromatography A*. 992(1–2): 1–9.
[8] C. Gonçalves, and M. F. Alpendurada. 2005. Assessment of Pesticide Contamination in Soil Samples from an Intensive Horticulture Area, Using Ultrasonic Extraction and Gas Chromatography–mass Spectrometry. *Talanta*. 65(5): 1179–1189.

[9] K. V. Gobi, H. Tanaka, Y. Shoyama *et al*. 2005. Highly Sensitive Regenerable Immunosensor for Label-free Detection of 2,4-Dichlorophenoxyacetic Acid at Ppb Levels by Using Surface Plasmon Resonance Imaging. *Sensors and Actuators B: Chemical*. 111–112: 562–571

[10] D. R. Shankaran, K. V. Gobi, T. Sakai *et al*. 2005. Surface Plasmon Resonance Immunosensor for Highly Sensitive Detection of 2,4,6-Trinitrotoluene. *Biosensors and Bioelectronics*. 20(9): 1750–1756.

[11] T. Kawaguchi, D. R. Shankaran, S. J. Kim *et al*. 2007. Fabrication of a Novel Immunosensor Using Functionalized Self-assembled Monolayer for Trace Level Detection of TNT by Surface Plasmon Resonance. *Talanta*. 72(20): 554–560.

[12] S. Helali, H. B. Fredj, K. Cherif *et al*. 2008. Surface Plasmon Resonance and Impedance Spectroscopy on Gold Electrode for Biosensor Application. *Materials Science and Engineering: C*. 28(5–6): 588–593.

[13] G. Lindergard, S. E. Wade, S. Schaaf *et al*. 2001. Detection of Cryptosporidium Oocysts in Soil Samples by Enzyme-linked Immunoassay. *Veterinary Parasitology*. 94(3): 163–176.

[14] M. Nording, K. Frech, Y. Persson *et al*. 2006. On the Semi-quantification of Polycyclic Aromatic Hydrocarbons in Contaminated Soil by an Enzyme-linked Immunosorbent Assay Kit. *Analytica Chimica Acta*. 555(1): 107–113.

[15] J. M. V. Emon, J. C. Chuang, R. A. Lordo *et al*. 2008. An Enzyme-linked Immunosorbent Assay for the Determination of Dioxins in Contaminated Sediment And Soil Samples. *Chemosphere*. 72(1): 95–103.

[16] X.-X. Jiang, H.-Y. Shi, N. Wu. *et al*. 2011. Development of an Enzyme-Linked Immunosorbent Assay for Diniconazole in Agricultural Samples. *Food Chemistry*. 125(4): 1385–1389.

[17] G. S. Nunes, I. A. Toscano, and D. Barceló. 1998. Analysis of Pesticides in Food and Environmental Samples by Enzyme-linked Immunosorbent Assays. TrAC Trends in Analytical Chemistry. 17(2): 79–87.

[18] S. Camou, A. Shimizu, T. Horiuchi, and T. Haga. 2009. Ppt-level Aqueous Benzene Detection with an UV-spectroscopy based Portable Sensor. In Sensors, IEEE. 2021–2024.

[19] N. C. Filho, E. S. Medeiros, S. T. Tanimoto, and L. H. C. Mattoso. 2005. Sensors of Conducting Polymers for Detection of Pesticides in Contaminated Water. In Electrets, 2005. ISE-12. 2005 12th International Symposium. 424–427.

[20] S. S. Freeborn, J. Hannigan, and H. A. MacKenzie. A Portable Pulsed Photoacoustic Sensor for the Monitoring of Hydrocarbons in Process Water. IEE Colloquium on Optical Techniques for Environmental Monitoring. 1–3.

[21] V. Furtula, H. Osachoff, G. Derksen *et al*. 2012. Inorganic Nitrogen, Sterols and Bacterial Source Tracking as Tools to Characterize Water Quality and Possible Contamination Sources in Surface Water. *Water Research*. 46(40): 1079–1092.

[22] Y. Hanazato, M. Nakako, S. Shiono *et al*. 1989. Integrated Multi-biosensors Based on an Ion-sensitive Field-effect Transistor Using Photolithographic Techniques. *Electron Devices, IEEE Transactions on*. 36(7): 1303–1310.

[23] P. Nikitin, A. Kabashin, T. Ksenevich, and N. Kalabina. 1997. Bio-Optoelectronical “tongue” for Detection of Pesticide Contamination of Water. In Solid State Sensors and Actuators. Transducers. '97 Chicago, 1997 International Conference on. 1: 495–497.

[24] M. G. Schweyer, J. C. Andle, D. J. McAllister, and J. F. Vetelino. 1996. An Acoustic Plate Mode Sensor for Aqueous Mercury. *Sensors and Actuators B: Chemical*. 35: 170–175.

[25] C. Gooneratne, S. C. Mukhopadhyay, and S. Yamada. 2005. Novel Planar Electromagnetic Sensors-Characterization and Comparative Evaluation. In Magnetics Conference, 2005. INTERMAG Asia 2005. Digests of the IEEE International. 965–966.

[26] S. Mukhopadhyay. 2005. Novel Planar Electromagnetic Sensors: Modeling and Performance Evaluation. *IEEE Sensors Journal*. 5(12): 546–579.

[27] M. A. Md Yunus, S. C. Mukhopadhyay, and S. Ibrahim. 2012. Planar Electromagnetic Sensor Based Estimation of Nitrate Contamination in Water Sources Using Independent Component Analysis. *IEEE Sensors Journal*. 12(6): 2024–2034.

[28] M. A. M. Yunus and S. C. Mukhopadhyay. 2011.Development of Planar Electromagnetic Sensors for Measurement and Monitoring of Environmental Parameters. *Measurement Science and Technology*. 22: 025107.

[29] M. A. Md Yunus and S. C. Mukhopadhyay. 2011. Novel Planar Electromagnetic Sensors for Detection of Nitrates and Contamination in Natural Water Sources. *Sensors Journal, IEEE*. 11: 1440–1447.